International Journal for Housing Science and Its Applications
Publish August 6, 2025. Volume 46, Issue 3 Pages 8417-8425

https://doi.org/10.70517/ijhsa463720

Multivariate statistics and isotope technology combined evolutionary mechanism of water chemistry processes in the Anle Village mining area

Huiqian Zhang[1], Dongchuan Xue[1,*], Jiahui Zhang[1] and Li Wang[1]
[1] Faculty of Land Resources Engineering, Kunming University of Science and Technology, Kunming, Yunnan, 650093, China
Corresponding authors: (e-mail: hannibalnn@163.com).

Abstract Taking Anle Village mining area as the research object, this paper systematically analyzes the spatial and temporal differentiation characteristics of the chemical components of groundwater and surface water under the influence of mining activities and their driving mechanisms by integrating the hydrogeological model and artificial intelligence algorithms. A three-dimensional hydrogeological model was constructed based on the measured data of 45 groups of water samples collected in 2024. Combining geostatistics and machine learning methods to optimize the parameter estimation, the model was solved by the finite unit method to verify the accuracy. It is found that the surface water and groundwater in the mining area show significant differences in chemical components, and the mean values of the mass concentrations of major ions in the surface water are higher than those in the groundwater, except for NO_3^- and pH. The hydrochemical evolution is dominated by carbonate rock weathering, supplemented by silicate rock dissolution contributions, and cation exchange shows directional differences. Soil moisture has a significant positive correlation with groundwater level fluctuations, but there is a phase difference of 15-30 days. This paper confirms that the multi-source data fusion model can effectively reveal the dynamic evolution law of hydrochemical processes under the complex geological environment, and provide a scientific basis for the sustainable utilization of water resources in mining areas.

Index Terms groundwater, surface water, hydrogeological model, finite unit method, hydrochemical evolution

I. Introduction

The hydrogeological conditions of the mining area are extremely complex, and the complex groundwater system composed of surface water and groundwater poses a certain threat to the safe production in the mining area, and also restricts the rational development and utilization of regional water resources to a certain extent [1]. Due to the different lithology of different aquifers, their permeability and water content are very different, and the spatial distribution and depositional characteristics of regional aquifers determine their recharge, runoff and discharge characteristics [2], [3]. Especially under the disturbance of human engineering activities such as mineral mining, the conditions of groundwater runoff, discharge and hydrogeochemical characteristics of the mining area have been changed to a certain extent [4], [5].

On the other hand, Anle Village is rich in mineral resources, and many pollutants will be generated during the mining process, which will cause serious pollution of the surrounding soil and water bodies, and the threat to karst groundwater will be even greater [6], [7]. For this reason, on the basis of the analysis of the hydrogeological conditions of the Anle Village mining area, a large number of boreholes and hydrogeological profiles in the mining area were collected, a three-dimensional geological structure model of the mining area was established, and the changing law of the water level and volume of groundwater was analyzed [8]-[10]. The hydrochemical characteristics of each aquifer were systematically studied, the age of groundwater was constrained, and the hydrogeochemical processes and influencing factors were simulated [11], [12]. And on the basis of hydrogeological modeling, the hydrogeological characteristics, spatial distribution law and hydrochemical processes of the aquifer system in the mining area can effectively reveal the evolution mechanism of groundwater in the coal mine area, and provide technical support for the identification of the water source in the safe production of the mining area and the development and utilization of regional groundwater resources, which is both of theoretical significance and practical value [13]-[15].

In this paper, surface water, quaternary groundwater and mine water in Anlecun mining area were firstly sampled and tested, and the testing indexes included water quality routine indexes and toxicological indexes. In the BoreholeData module, we imported and managed the borehole data, and selected the permeability coefficient, water storage coefficient, and water release coefficient to construct the hydrogeological model. The finite element method was used to solve the model, and the accuracy of the model was evaluated by comparing the simulation results with the actual observation data. The basic characteristics of the hydrochemical components are analyzed, and the hydrochemical types are revealed by Piper's trilinear diagram. Based on the multivariate statistical analysis, the evolution mechanism of the hydrochemical components and the groundwater-surface water interaction mechanism are investigated.

II. Hydrogeological modeling of the Anlecun mining area

As an important base for regional resource development, the evolution of the chemical components of groundwater and surface water in the Anlecun mining area has a profound impact on the ecological environment and the sustainability of water resources in the mining area. Tailings discharge, acid mine drainage and aquifer structure disturbance triggered by mining activities have significantly altered the chemical balance of the water-rock-microbial system, resulting in significant spatial and temporal heterogeneity in the chemical characteristics of groundwater and surface water.

II. A.Water Sample Collection and Testing Methods

In 2024, two batches of water samples from different water bodies were collected from the main well fields of the Anlak village mining area, totaling 45 groups, including 13 groups of winter water samples and 32 groups of summer water samples, including 12 groups of surface water samples, 13 groups of fourth system groundwater samples, and 20 groups of mine water samples. Winter water samples included 4 groups of surface water samples, 4 groups of fourth system groundwater samples, and 5 groups of mine water samples, while summer water samples included 6 groups of surface water samples, 15 groups of fourth system groundwater samples, and 24 groups of mine water samples. The collected water samples were filtered by 0.6μm polyethersulfone membrane and divided into two parts, which were analyzed and tested for cations and anions respectively, and sent to the Geochemical Laboratory of the local Institute of Chemistry for water quality testing under sealed and lightproof conditions, and the testing items included general water chemistry indexes (pH, TDS, HCO_3^-, SO_4^-, Cl^-, F^-, NO_3^-, Na^+, K^+, Ca^{2+}, Mg^{2+}, Fe, and Mn) and toxicological indicators (As, Cr^{6+}, Cd, Pb, and Hg). The pH of the water samples was determined in the laboratory by the glass electrode method; TDS in the water samples was determined by the evaporation method; HCO_3^- in the water samples was determined by the titration method; the other anions in the water samples were determined by the ion chromatography method; the general cations in the water samples were determined by the flame atomic absorption spectrophotometric method; and the toxicological indicators of the water samples were determined by the inductively coupled plasma Inductively coupled plasma mass spectrometry was used for the determination of toxicological indicators. All the macronutrients of water samples passed the charge balance test with an error of less than 3%.

II. B.Hydrogeologic modeling methods

II. B. 1) Hydrogeologic modeling in the Borehole module

(1) Importing geographic base maps and setting the coordinate system: First, geographic base maps need to be imported into GMS. This usually involves the import of a GIS file, such as a shapefile or GeoTIFF format file. Once the basemap has been imported, the next step is to set up the exact coordinate system.GMS supports a variety of coordinate systems, including UTM, Lambert Conformal Conic, Mercator, and others. It is critical to select a coordinate system that matches the base map to ensure that subsequent data is displayed correctly on the map. This step is the foundation of the entire modeling process, and the wrong coordinate system will lead to data misalignment and affect the accuracy of the model.

(2) Sketch operational area boundaries and construct irregular triangular networks (TINs): In the mapping module, operational area boundaries are manually drawn on the geographic base map using drawing tools. The boundaries can be natural terrain features, such as rivers and mountains, or artificially delineated areas, such as administrative boundaries. Once the boundaries are identified, these boundary points are used to construct irregular triangular networks (TINs).TINs are digital models used to represent continuous surfaces that simulate the surface or other interfaces by connecting adjacent points to form non-overlapping triangles. In this process, the step size of spatial interpolation, i.e. the size of each triangle, needs to be determined, which will directly affect the accuracy of subsequent interpolation and the resolution of the model.

(3) Organize borehole information and generate borehole data: Collect on-site borehole information, including borehole location, depth, and stratigraphic information. These data are organized into a format recognizable by GMS, and the data will be imported into the Borehole module. In this module, the user can view and manage all the borehole data, which provides the necessary information for building the hydrogeological model.

(4) Creating hydrogeological structure solids and constructing the model: In the Borehole module, Horizons→ Solid commands are used to generate hydrogeological structures. This step involves choosing appropriate

interpolation methods, such as Kriging interpolation, distance inverse weighted interpolation, etc., to infer the stratigraphic distribution of the unknown area based on the borehole data. The interpolation results will form one or more 3D entities representing different hydrogeologic units. These entities can be further analyzed and visualized to build a complete hydrogeological model.

II. B. 2) Parameter Selection and Estimation

In hydrogeological modeling, the selection and estimation of parameters are crucial, and they directly affect the accuracy and reliability of the model. The following is the detailed process of parameter selection and estimation.

(1) Parameter Selection

a) Permeability coefficient (K). Permeability coefficient is a parameter describing the ability of fluid to pass through porous media, and its selection is usually based on the laboratory test results of core samples. The selection of permeability coefficient needs to consider the lithology of different aquifers, the degree of fracture development and other factors, and its expression is:

$$K = \frac{k\rho g}{\mu} \tag{1}$$

where, K is the permeability, ρ is the fluid density, g is the gravitational acceleration, and μ is the dynamic viscosity of the fluid.

b) Water storage coefficient (S). The water storage coefficient is a dimensionless parameter that describes the ability of an aquifer to store water when subjected to head changes. The estimation of the water storage coefficient is usually based on the relationship between the change in water level and the change in water influx, and its expression is:

$$S = \frac{\Delta Vw}{\Delta H \cdot A} \tag{2}$$

where, ΔVw is the change in aquifer storage volume, ΔH is the change in head, and A is the aquifer area.

c) Water release coefficient (T). The water release coefficient is a parameter that describes the amount of water released from the aquifer when the unit head is reduced. Its estimation can be obtained by pumping test and the expression is:

$$T = \frac{Q}{4\pi H} \tag{3}$$

where, Q is the pumping volume and H is the radius of influence of pumping.

(2) Parameter estimation

a) Geostatistical methods: geostatistical methods can be used to estimate hydrogeological parameters using spatial variability and structural features. Semi-variance function and Kriging interpolation are commonly used geostatistical methods. The semi-variational function can describe the spatial variability of parameters with the formula:

$$\gamma(h) = \frac{1}{2N(h)} \sum_{i=1}^{N(h)} \left[Z(x_i) - Z(x_i + h) \right]^2 \tag{4}$$

where, $\gamma(h)$ is the semi-variance value, h is the lag distance, $Z(x_i)$ and $Z(x_i + h)$ are the parameter values at locations x_i and $x_i + h$, respectively, and $N(h)$ is the number of pairs of data with a lag distance of h.

b) Machine learning methods: machine learning methods, such as artificial neural networks (ANN) and support vector machines (SVM), can be used to estimate hydrogeological parameters. Take artificial neural network as an example, its basic structure includes input layer, hidden layer and output layer. The parameter estimation process can be expressed as:

$$Output = f\left(W \cdot X + b\right) \tag{5}$$

where, X is the input vector, W is the weight matrix, b is the bias vector, and f is the activation function.

Through the above methods, the parameters of the coal mine hydrogeological model under the complex geological environment can be estimated more accurately, so as to improve the prediction ability of the model. In practice, it may be necessary to combine the specific geological conditions and hydrogeological features of the mining area to make appropriate adjustments and optimizations to the above methods.

II. B. 3) Model Solving and Validation

After constructing the hydrogeological model, it is necessary to solve the model through numerical simulation methods and verify the accuracy of the model through actual observation data.

(1) Model solving

Numerical simulation methods mainly include the finite-difference method (FDM), finite-element method (FEM) and boundary-element method (BEM). The following is an example of the finite element method to illustrate the model solving process.

The finite element method discretizes the continuous solution domain into a finite number of elements, and transforms the continuous partial differential equations into a set of algebraic equations through the variational principle or the weighted residual method. For groundwater flow problems, the commonly used governing equations are Darcy's law and the continuity equation.

Darcy's law is expressed as:

$$q = -K\nabla h \tag{6}$$

where q is the Darcy velocity, K is the permeability coefficient tensor, and h is the head.

The continuity equation is expressed as:

$$\nabla \cdot q + Q = 0 \tag{7}$$

where, Q is the source-sink term.

After discretizing the above equations, the following system of linear equations can be obtained:

$$[K]\{h\} = \{Q\} \tag{8}$$

where, K is the overall permeability coefficient matrix, $\{h\}$ is the nodal head vector, and $\{Q\}$ is the source-sink term vector. By solving the system of equations, the groundwater head at each node can be obtained.

Solving the above system of linear equations is usually done by an iterative method, such as the Gauss-Seidel iterative method or the conjugate gradient method. The basic iterative formula for the conjugate gradient method is:

$$p_k = r_k + \beta_k p_{k-1} \tag{9}$$

$$\alpha_k = \frac{r_k^T r_k}{p_k^T A p_k \Delta x} \tag{10}$$

$$x_k = x_{k-1} + \alpha_k p_k \tag{11}$$

$$r_{k+1} = r_k - \alpha_k A p_k \tag{12}$$

where, p_k is the search direction, r_k is the residual, α_k and β_k are the step size and direction adjustment coefficients, x_k is the k th iteration solution, and A is the coefficient matrix for the system of linear equations.

(2) Model validation

Model validation refers to the process of assessing the accuracy of the model by comparing the simulation results with the actual observed data.

a) Fit indicators: commonly used fit indicators include root mean square error (RMSE) and coefficient of determination $\left(R^2\right)$.

The expression for root mean square error is:

$$RMSE = \sqrt{\frac{1}{n}\sum_{i=1}^{n}(h_{sim,i} - h_{obs,i})^2} \tag{13}$$

where $h_{sim,i}$ is the simulated head, $h_{obs,i}$ is the observed head, and n is the number of data points.

The expression for the coefficient of determination is:

$$R^2 = 1 - \frac{\sum_{i=1}^{n}(h_{sim,i} - h_{obs,i})^2}{\sum_{i=1}^{n}(h_{obs,i} - \overline{h}_{obs})^2} \tag{14}$$

where, $\overline{h}_{obs}$ is the average value of the observed head.

b) Validation process: first, the model is made to run under the initial conditions to obtain the simulation results. Then, compare with the actual observed data and calculate the fit index. If the fit does not satisfy the preset criteria, the model parameters or structure need to be adjusted and the simulation needs to be repeated until the simulation results reach a satisfactory fit with the observed data. Through the above process, it can be ensured that the hydrogeological model provides accurate prediction and effective decision support in the safe production of coal mines under complex geological environment.

III. Study of the mechanism of evolution of hydrochemical processes in groundwater and surface water in the Anlecun mining area

III. A. Basic characteristics of water chemistry

Statistical analysis can provide a preliminary understanding of the basic characteristics of the hydrochemical components and help to recognize the hydrochemical genesis. The hydrochemical statistical results of surface water and groundwater in Anlecun mining area are shown in Table 1. Where TH is total hardness and TDS is total dissolved solids.

In surface water, the cation mass concentration relationship was $\rho\left(\mathrm{Na}^+ + \mathrm{K}^+\right) > \rho\left(\mathrm{Ca}^{2+}\right) > \rho\left(\mathrm{Mg}^{2+}\right)$, with mean values of 123.57, 66.23, 21.05mg/L, respectively; the anion mass concentration relationship was $\rho\left(\mathrm{HCO}_3^-\right) > \rho\left(\mathrm{SO}_4^{2-}\right) > \rho\left(\mathrm{Cl}^-\right) > \rho\left(\mathrm{NO}_3^-\right)$, with mean values of 262.18, 176.92, 80.35, 4.04mg/L, respectively. pH value of surface water ranged from 8.06 to 8.87, with a mean value of 8.11, which was weakly alkaline water. In the groundwater, the cation mass concentration existed the characteristics of $\rho\left(\mathrm{Na}^+ + \mathrm{K}^+\right) > \rho\left(\mathrm{Ca}^{2+}\right) > \rho\left(\mathrm{Mg}^{2+}\right)$, the mean values were 70.22, 59.66, 14.73mg/L, and the difference between the mean values of $\mathrm{Na}^+ + \mathrm{K}^+$ and Ca^{2+} was small; the relationship between the anion mass concentration was $\rho\left(\mathrm{HCO}_3^-\right) > \rho\left(\mathrm{SO}_4^{2-}\right) > \rho\left(\mathrm{Cl}^-\right) > \rho\left(\mathrm{NO}_3^-\right)$, the mean values were 232.74, 63.35, 53.18, and 6.11mg/L. The pH of the groundwater ranged from 7.27 to 8.96, the mean value was 8.16, which it is weakly alkaline water. Comparison can be seen: except for NO_3^- and pH value, the average value of the mass concentration of major ions in surface water is higher than that of groundwater.

The coefficient of variation is the ratio of the standard deviation to the mean, reflecting the degree of dispersion on the unit mean. As can be seen from Table 1, in surface water, the coefficients of variation of each component are small, among which the maximum of $NO3^-$ is 0.52, which indicates that the main chemical components in surface water are relatively stable and have a single chemical action. In groundwater, except for pH, TDS and $HCO3^-$, the coefficients of variation are smaller, the rest are higher than 0.50, indicating that the spatial variation of chemical components in groundwater is obvious, which is mainly due to the different sampling depths and stratigraphic positions of groundwater. On the whole, there are some differences in the characteristics of the hydrochemical composition of surface water and groundwater.

III. B. Types of water chemistry

Piper trilinear diagrams are widely used in water chemistry studies. The results of the Piper analysis of surface water and groundwater in the Anlecun mining area are shown in Figure 1. Among them, the lower left and lower right triangles indicate the milligram equivalents (mM x valence) percentages of cations and anions, respectively, and the projection into the diamonds indicates the relative contents of anions and cations. As can be seen in Fig. 1, there are differences in water chemistry types between surface water and groundwater in different distribution areas. Based on the Piper diagram, the fourth system groundwater belongs to HCO_3-Ca type water, the mine water sample is Cl-Na type water, and the surface water contains these 2 types. As a whole, the water samples can be divided into 3 regions, in which the distribution regions of surface water and the fourth system groundwater are closer to each other, indicating that there is a certain hydraulic connection between them. The mine water samples were sampled at a relatively deeper depth, and the distribution area was obviously different from the other water samples, indicating that the connection between mine water and the fourth system groundwater and surface water was relatively weak.

Table 1: Summary of Statistical Results of Water chemical Components

Type of water sample	Metrics	pH	Mass concentration/(mg·L^{-1})								
			K^++Na^+	Ca^{2+}	Mg^{2+}	Cl^-	SO_4^{2-}	HCO_3^-	TH	TDS	NO_3^-
Surface water	Max	8.87	136.28	75.32	30.18	95.44	233.65	282.17	301.38	636.28	6.04
	Min	8.06	62.91	58.14	20.11	32.64	112.77	183.95	182.47	378.66	2.06
	Mean	8.11	123.57	66.23	21.05	80.35	176.92	262.18	266.94	601.78	4.04
	SD	0.12	51.26	11.35	6.15	25.28	46.77	54.26	50.19	163.34	1.16
	CV	0.03	0.48	0.21	0.37	0.46	0.19	0.28	0.24	0.33	0.52
Groundwater	Max	8.96	196.31	96.25	26.78	98.75	128.44	296.83	499.15	494.63	9.18
	Min	7.27	13.47	2.21	0.32	9.86	21.42	132.89	6.17	271.08	0.02
	Mean	8.16	70.22	59.66	14.73	53.18	63.35	232.74	183.28	399.71	6.11
	SD	0.63	68.96	30.25	8.09	36.17	31.19	57.19	123.47	79.26	8.25
	CV	0.11	0.65	0.66	0.66	0.79	0.64	0.32	0.78	0.44	2.07

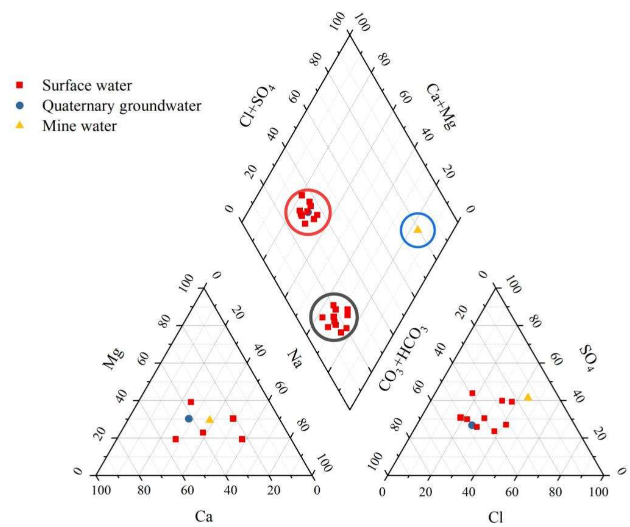

Figure 1: Results of Piper analysis of surface and groundwater

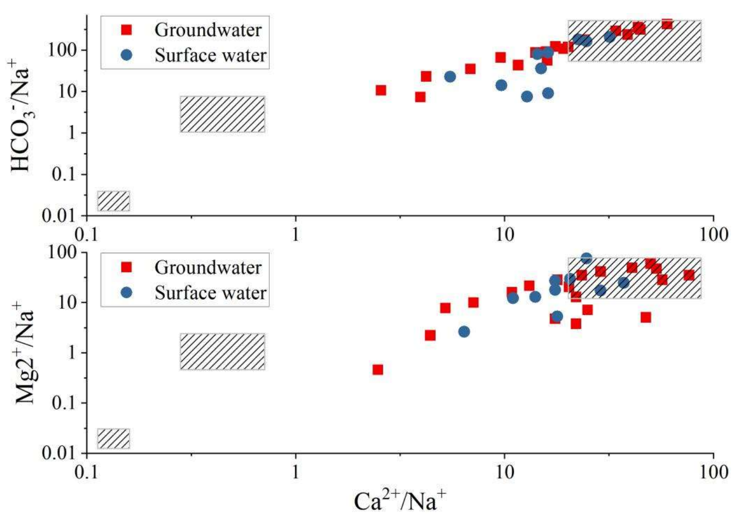

Figure 2: Relationship between groundwater and surface water components

III. C. Mechanisms of water chemistry evolution

Factors such as atmospheric precipitation, regional geologic formations, hydrodynamic conditions, and human activities collectively influence groundwater chemical characteristics, and in turn, water chemistry characteristics store and reverse the above complex information. The relationship between the chemical components of groundwater and surface water in the study area is shown in Figure 2. The groundwater and surface water samples are mainly distributed in the area of carbonate rock dissolution end-element, and some samples are close to the silicate rock end-element, and there is a tendency to extend to the direction of silicate rock, which indicates that the hydrogeochemical processes in the study area are mainly controlled by the weathering and dissolution of carbonate rock, and at the same time, the weathering and dissolution of mineralization of silicate rock (feldspars, etc.) also have some contribution, which is attributed to the fact that the study area is mainly dominated by carbonate rock.

The main process by which cation exchange occurs in the water column is the ion exchange of Ca^{2+} and Mg^{2+} with Na^{+} and K^{+} on the surface of the aquifer rocks, which results in an increase of Na^{+} and K^{+} and a relative decrease of Ca^{2+} and Mg^{2+} decrease relatively, and the corresponding $Na^{+}/(Na^{+}+Cl^{-})$ (volume-concentration ratio) should be greater than 0.5. The relationship between the cation exchange effect of the groundwater and the surface water and the chlor-alkali index is shown in Figure 3. The values of $Na^{+}/(Na^{+}+Cl^{-})$ of groundwater and surface water in the zone are mostly distributed near 0.5, indicating that the cation exchange effect occurred is not obvious, and only a very small part of the water points have cation exchange effect. As to whether cation exchange occurs in the water body and to further judge the strength and direction of cation exchange, the chlor-alkali indices (CA-I and CA-II) can be used to study, usually, when positive cation exchange occurs, the values of CA-I and CA-II are less than 0, and on the contrary, the values of CA-I and CA-II are greater than 0. 90.2% of the chlor-alkali indices of the groundwater samples are negative, which indicates that positive cation exchange mainly occurs in the groundwater. 90.2% of the groundwater samples had negative chlor-alkali indices, indicating that positive cation exchange mainly occurred in the groundwater, which led to an increase in the contents of Na^{+} and K^{+}, and a relative decrease in the contents of Ca^{2+} and Mg^{2+}, whereas the chlor-alkali indices of the surface water were negative, indicating that positive cation exchange mainly occurred in the groundwater.

$$\mathrm{CA-I} = N\left(\mathrm{Cl} - \mathrm{Na}^{+} - \mathrm{K}^{+}\right) / N\left(\mathrm{Cl}^{-}\right) \tag{15}$$

$$\mathrm{CA^{-}II} = N\left(\mathrm{Cl} - \mathrm{Na}^{+} - \mathrm{K}^{+}\right) / N\left(\mathrm{SO_4^{2-}} + \mathrm{HCO_3^{-}} + \mathrm{CO_3^{2-}} + \mathrm{NO_3^{-}}\right) \tag{16}$$

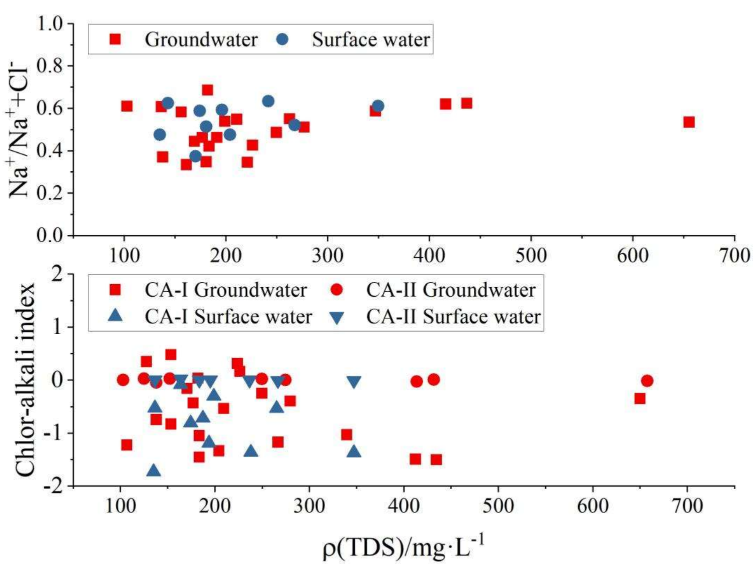

Figure 3: Relationship between cation exchange and chlor-alkali index

III. D. Analysis of soil moisture and water table fluctuations

The curves of the relationship between soil moisture and water level in the boreholes in 2024 at the Anle Village mine are shown in Fig. 4. The water level in the monitoring boreholes from January to May 2024 showed relatively small changes. However, after June 2024, the water level in the monitoring boreholes gradually increased to 3918 m. The water level elevation in the monitoring boreholes was the largest in September 2024, about 3966 m. And the water level elevation in the monitoring boreholes decreased to the smallest in December 2024, about 3848 m, with a fluctuating range of about 118 m. From January to March is the dry season, and the water level in the boreholes rapidly decreased to a certain level and stayed unchanged. And after March, after snow melting and rainy season, the water level keeps recovering to a higher level. And September is the rainy season, the water level in the borehole is generally higher. Comparative analysis of the soil moisture and borehole water level curves shows that the two trends are basically the same, with an obvious positive correlation compared to the soil moisture changes to be 15-30 days ahead of the borehole water level changes.

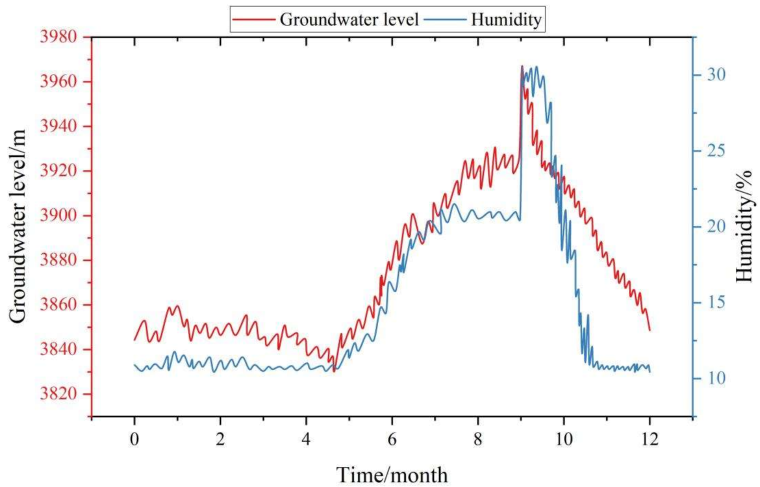

Figure 4: Relationship between soil moisture and borehole water level

IV. Conclusion

In this paper, a hydrogeological model of the Anlecun mining area was constructed using the 2024 drilling data of the area. Combined with artificial intelligence algorithms to solve the model, to explore the evolution mechanism of the hydrochemical processes of groundwater and surface water in the Anlecun mining area.

(1) The hydrochemical components show significant spatial differentiation.

In surface water, the cation mass concentration relationship is $\rho\left(\mathrm{Na}^{+}+\mathrm{K}^{+}\right)>\rho\left(\mathrm{Ca}^{2+}\right)>\rho\left(\mathrm{Mg}^{2+}\right)$, and the anion mass concentration relationship is $\rho\left(\mathrm{HCO}_3^{-}\right)>\rho\left(\mathrm{SO}_4^{2-}\right)>\rho\left(\mathrm{Cl}^{-}\right)>\rho\left(\mathrm{NO}_3^{-}\right)$, which is weakly alkaline water. In the groundwater, there is a cation mass concentration of $\rho\left(\mathrm{Na}^{+}+\mathrm{K}^{+}\right)>\rho\left(\mathrm{Ca}^{2+}\right)>\rho\left(\mathrm{Mg}^{2+}\right)$ is characterized by an anion mass concentration relationship of $\rho\left(\mathrm{HCO}_3^{-}\right)>\rho\left(\mathrm{SO}_4^{2-}\right)>\rho\left(\mathrm{Cl}^{-}\right)>\rho\left(\mathrm{NO}_3^{-}\right)$, is weakly alkaline water. In surface water, the coefficients of variation (CoVs) of each component were small, with the maximum of 0.52 for $NO3^{-}$. In groundwater, all of them were higher than 0.50, except for pH, TDS, and $HCO3^{-}$, which were smaller.The groundwater of the fourth system was of the HCO_3-Ca type of water, and the water samples from the mines were of the Cl-Na type of water, and the surface water contained these 2 types. On the whole, the water samples can be divided into three regions, in which the distribution areas of surface water and the fourth system groundwater are closer to each other, and the connection between the mine water and the fourth system groundwater and surface water is relatively weak.

(2) Evolutionary mechanism of hydrochemical processes

The groundwater and surface water samples are mainly distributed in the area of dissolved carbonate rock end-elements, and some samples are close to the silicate rock end-elements, and there is a tendency to extend in the direction of silicate rock. The cation exchange between groundwater and surface water in the area is not obvious, and positive cation exchange mainly occurs in the groundwater, while the chlor-alkali index of surface water is negative, indicating that positive cation exchange mainly occurs in it. The water level in the monitoring boreholes in the Anlecun mine area varied little from January to May 2024, and gradually increased to 3918m in June 2024, with a maximum elevation of 3966m in September 2024, and a minimum elevation of 3848m in December 2024, with a fluctuating range of about 118m.

References

[1] Keqiang, H., Lu, G., Yuanyuan, G., Huilai, L., & Yongping, L. (2019). Research on the effects of coal mining on the karst hydrogeological environment in Jiaozuo mining area, China. Environmental Earth Sciences, 78(15), 434.

[2] Devy, S. D., & Sarungallo, C. (2018). Groundwater aquifer study on coal mining area: a case of North Samarinda, Indonesia. Journal of Degraded and Mining Lands Management, 6(1), 1483.

[3] Wang, C., Liao, F., Wang, G., Qu, S., Mao, H., & Bai, Y. (2023). Hydrogeochemical evolution induced by long-term mining activities in a multi-aquifer system in the mining area. Science of the Total Environment, 854, 158806.

[4] Huang, W., Sui, L., Wang, Y., Zhang, C., Jiang, D., Cai, X., & Yang, Z. (2023). Study of the mining and aquifer interactions in complex geological conditions and its management. Scientific Reports, 13(1), 9462.
[5] Qu, S., Wang, G., Shi, Z., Zhu, Z., Wang, X., & Jin, X. (2022). Impact of mining activities on groundwater level, hydrochemistry, and aquifer parameters in a Coalfield's overburden aquifer. Mine Water and the Environment, 41(3), 640-653.
[6] Liu, S., Li, W., Qiao, W., Li, X., Wang, Q., & He, J. (2019). Zoning method for mining-induced environmental engineering geological patterns considering the degree of influence of mining activities on phreatic aquifer. Journal of Hydrology, 578, 124020.
[7] Hou, Z., Huang, L., Zhang, S., Han, X., Xu, J., & Li, Y. (2024). Identification of groundwater hydrogeochemistry and the hydraulic connections of aquifers in a complex coal mine. Journal of Hydrology, 628, 130496.
[8] Wu, Q., & Xu, H. (2014). Three-dimensional geological modeling and its application in digital mine. Science China Earth Sciences, 57, 491-502.
[9] Wycisk, P., Hubert, T., Gossel, W., & Neumann, C. (2009). High-resolution 3D spatial modelling of complex geological structures for an environmental risk assessment of abundant mining and industrial megasites. Computers & Geosciences, 35(1), 165-182.
[10] Wang, Z., Tang, S., Yan, Z., Zhang, S., Xi, Z., Zhang, K., ... & Yang, X. (2023). Three-Dimensional geological modeling of coal reservoirs and analysis of sensitivity factors for combined mining capacity. Processes, 11(12), 3448.
[11] Che, D., & Jia, Q. (2019). Three-dimensional geological modeling of coal seams using weighted Kriging method and multi-source data. Ieee Access, 7, 118037-118045.
[12] Wang, J., Zhu, W., Li, H., Qin, T., & Zhou, M. (2025). Three-dimensional geological modeling of thin ore body and complex strata based on multi-point geostatistics. Engineering Geology, 352, 108056.
[13] Huang, H., Chen, Z., Wang, T., Zhang, L., Zhou, G., Sun, B., & Wang, Y. (2019). Characteristics and processes of hydrogeochemical evolution induced by long-term mining activities in karst aquifers, southwestern China. Environmental Science and Pollution Research, 26, 30055-30068.
[14] Zhan, H., Liu, S., Wu, Q., Liu, W., Shi, L., & Liu, D. (2024). Effects of deep coal mining on groundwater hydrodynamic and hydrochemical processes in a multi-aquifer system: Insights from a long-term study of mining areas in ecologically fragile western China. Journal of Contaminant Hydrology, 265, 104386.
[15] Qian, J., Tong, Y., Ma, L., Zhao, W., Zhang, R., & He, X. (2018). Hydrochemical characteristics and groundwater source identification of a multiple aquifer system in a coal mine. Mine Water and the Environment, 37(3), 528-540.